Liquid Crystals
Publication details, including instructions for authors and subscription information:
http://www.informaworld.com/smpp/title~content=t713926090

Adiabatic scanning calorimetry of the nematic-smectic A_1 and the smectic A_1-smectic A transitions in frustrated smectic mixtures at low temperatures

J. Thoen[a][b]; H. Beringhs[a]; J. M. Auguste[c]; G. Sigaud[c]
[a] Laboratorium voor Molekuulfysica, Katholieke Universiteit Leuven, Leuven, Belgium [b] Laboratorium voor Akoestiek en Warmtegeleiding, Katholieke Universiteit Leuven, Leuven, Belgium [c] Centre de Recherche Paul Pascal, Domaine Universitaire, Université de Bordeaux I, Talence Cedex, France

To cite this Article Thoen, J. , Beringhs, H. , Auguste, J. M. and Sigaud, G.(1987) 'Adiabatic scanning calorimetry of the nematic-smectic A_1 and the smectic A_1-smectic A transitions in frustrated smectic mixtures at low temperatures', Liquid Crystals, 2: 6, 853 — 863

To link to this Article: DOI: 10.1080/02678298708086341

URL: http://dx.doi.org/10.1080/02678298708086341

Liquid Crystals, 1987, Vol. 2, No. 6, 853–863

Adiabatic scanning calorimetry of the nematic–smectic A_1 and the smectic A_1–smectic $\tilde{A}$ transitions in frustrated smectic mixtures at low temperatures

by J. THOEN† and H. BERINGHS
Laboratorium voor Molekuulfysica, Katholieke Universiteit Leuven,
Celestijnenlaan 200 D, B – 3030 Leuven, Belgium

J. M. AUGUSTE and G. SIGAUD
Centre de Recherche Paul Pascal, Domaine Universitaire, Université de
Bordeaux I, 33405 Talence Cedex, France

(*Received 6 May 1987; accepted 21 May 1987*)

Phase diagram results and high resolution adiabatic scanning calorimetric data are presented for several binary mixtures of 4-cyanocyclohexyl-4′-*n*-butylcyclohexane and 1 amino-9-fluorenone showing smectic A_1 and smectic $\tilde{A}$ phases at low temperatures. Contrary to present theoretical expectations and experimental evidence for other systems, we find strongly first order nematic to smectic A_1 transitions with a latent heat of about 2 kJ/mol for all the mixtures investigated. The enthalpy change related to the smectic A_1 to smectic $\tilde{A}$ transitions is two orders of magnitude smaller and corresponds most likely to a fluctuation induced first order transition.

1. Introduction

Since the first report on phase transition between two smectic A phases in 1979 by Sigaud and co-workers [1], several new smectic A phases have been discovered and characterized structurally [2]. These new liquid crystal structures were found to occur in long polar molecules with three aromatic rings [2, 3]. A phenomenological model introduced by Prost [4] has been very successful in describing this complex smectic polymorphism [4–7]. It was noted that in addition to the conventional (non-polar) one dimensional density wave a second spatial periodicity may occur for molecules containing large dipole moments. The positions of the heads of the polar molecules with respect to the layer are also relevant. It turns out that for these frustrated smectic phases two incommensurate lengths, the molecular length and the pair length, are relevant. Two order parameters, one for the centres of mass density and the other for the long range dipole correlations normal to the layers, are introduced. Much of the experimentally observed complexity can be understood as arising from the conflict between the elastic terms and the order parameter coupling terms in the free energy expression of the model.

Recently Sigaud *et al.* [8] described a phase diagram of a particular binary mixture involving a polar rod mesogen (cyanobicyclohexyl) and an aminosubstituted polyaromatic molecule (1-amino-pyrene). They also found a smectic A polymorphism

---

† Present address: Laboratorium voor Akoestiek en Warmtegeleiding, Katholieke Universiteit Leuven, Celestijnenlaan 200 D, B – 3030 Leuven, Belgium.

(S_{A_1}, $S_{\tilde{A}}$, S_{A_2}) slightly above room temperature, which was previously obtained only with long (tri-aromatic) polar rods at much higher (above 100°C) temperatures [2]. The convenient temperatures of the various transitions and the fact that these compounds are commercially available make such systems very attractive for study because, if needed, large samples can be used.

Here we present the results of a high resolution calorimetric study of the nematic to smectic A_1 and the smectic A_1 to smectic $\tilde{A}$ phase transitions, which are observed in the related binary system of 4-cyanocyclohexyl-4′-*n*-butylcyclohexane (CCH4) with 1-amino-9-fluorenone (1A9F). The phase diagram measurements and the characterization of the different phases have been carried out in Talence and the calorimetric measurements have been done in Leuven.

2. Phase diagram

The isobaric (1 atm) phase diagram of CCH4 and 1A9F is reproduced in figure 1. The compound CCH_4 (4-cyanocyclohexyl-4′-*n*-butylcyclohexane)

is nematic from 55°C to 79°C and presents upon cooling a monotropic smectic B phase below 53°C. The compound 1A9F (1-amino-9-fluorenone)

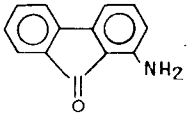

is not mesogenic at all and melts directly into an isotropic liquid at 119°C. The CCH4 was obtained from Merck and the 1A9F from Aldrich; both substances were used without further purification. The part of the phase diagram in figure 1 which involves the liquid-crystalline phases has been established by optical polarizing microscopy and differential scanning calorimetry (D.S.C.). The nature of the different smectic phases has been characterized by X-ray scattering.

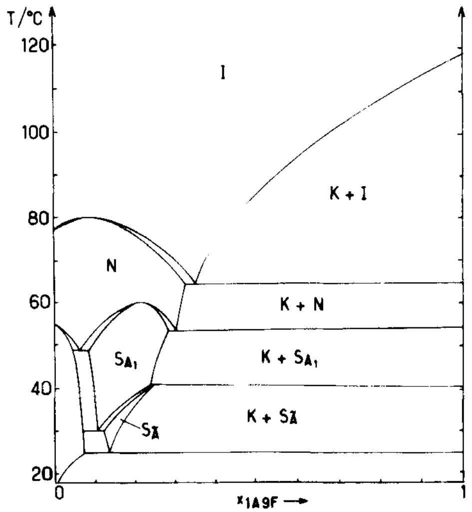

Figure 1. Isobaric phase diagram (p = 1 atm) for the system CCH_4 (left)—1-amino-9-fluorenone (right).

This system confirms the unusual phase behaviour previously observed for CCH4 with aminopyrene ($NH_2\pi$) [8]. Mesomorphic mixtures for the mole fraction x_{1A9F} up to about 0·3 can be obtained. Above that value demixing occurs and solid 1A9F precipitates when the temperature is decreased. Despite the strong shape differences between the two components, the nematic phase has an increased stability for $x_{1A9F} < 0{\cdot}08$ (figure 1). Unlike the CCH4–$NH_2\pi$ system [8] there is not a large S_{A_2} region present here. The dominant smectic phase in this case is a S_{A_1} phase, i.e. with a layer spacing close to one molecular length. Below this S_{A_1} phase there is, however, also a bidimensional $S_{\tilde{A}}$ phase with local bilayer S_{A_2} order and long range modulation [2]. The N–S_{A_1} equilibrium curve exhibits a maximum for $x_{1A9F} \simeq 0{\cdot}2$. This corresponds to a ratio of one amino molecule to four CCH4 molecules indicating some kind of complex formation which adds to the stabilization of the lamelar uniaxial phase [8].

In the phase diagram of figure 1, biphasic regions (thus assuming first order transitions) are indicated for both the N–S_{A_1} and the S_{A_1}–$S_{\tilde{A}}$ transitions. The assumption of the first order nature of these transitions was based on changes observed under the polarizing microscope and on D.S.C. results. Although it is known [9, 10] that in some cases this may lead to erroneous conclusions, here it is consistent with the high resolution adiabatic calorimetric results presented in the following section.

3. Calorimetric results

The measurements have been carried out with the same adiabatic scanning calorimeter as described earlier [10, 11]. A sample cell [12] with a maximum volume of 10 cm³ was filled with samples of between 5 and 8 g. Heating as well as cooling runs at very slow scanning rates, typically of the order of 30 mK/h, have been carried out. With a constant heating (cooling) power, P, applied to the sample, the experimental curve of temperature versus time, $T(t)$, results directly in the enthalpy of the sample [10]:

$$H(T) = H(T_s) - P(t - t_s), \tag{1}$$

where the index s refers to the starting conditions of the run. The heat capacity $C_p(T)$ is given by

$$C_p = P/\dot{T}. \tag{2}$$

$\dot{T}$ can be obtained by numerical differentiation from the direct experimental $T(t)$ data. In addition to the temperature dependence of the enthalpy and the heat capacity, it is also possible to obtain values for latent heats when they are present. If a first order transition occurs at T_1 between T_s and T, the temperature will be essentially constant for a time interval $\Delta t = \Delta H(T_1)/P$ with ΔH the latent heat. For mixtures we do not expect the transitions to take place at a single temperature T_1 but over a finite temperature range $\Delta T = T_f - T_i$. Even for nominally single component systems we observe a slight impurity broadening of first order transitions [10].

3.1. *The nematic–smectic A_1 transition*

For the nematic to smectic A_1 transition, measurements have been carried out for five different mixtures with mole fractions of 1A9F between 0·12 and 0·21. In each case results were obtained over temperature ranges between a few degrees below and a few degrees above the transition temperature. Cooling and heating runs with $\dot{T}$

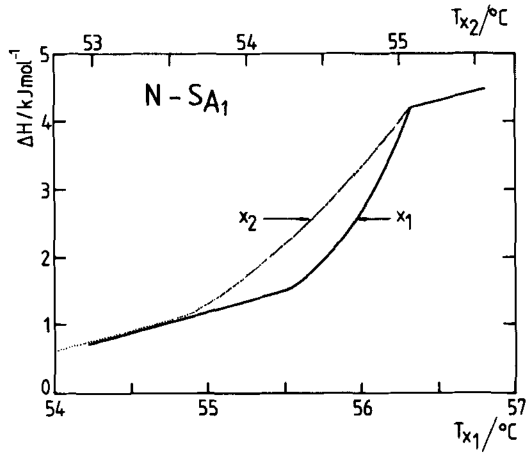

Figure 2. Temperature dependence of the enthalpy change $\Delta H = H(T) - H(T_s)$ (equation (1)) near the nematic to smectic A_1 transitions for two different mixtures of CCH_4 and 1A9F. The temperature scale at the top of the figure applies for mixture $x_2 = x_{1A9F} = 0{\cdot}1230$ and the bottom one for mixture $x_1 = x_{1A9F} = 0{\cdot}1558$.

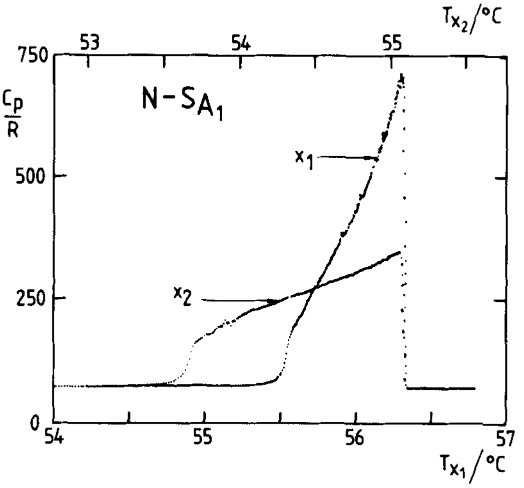

Figure 3. Results for the reduced molar heat capacity C_p/R derived from the enthalpy data given in figure 2.

values between 0·03 K/h and 0·07 K/h gave, in all cases, essentially the same results. In figure 2 the enthalpy change versus temperature is given for two different mixtures ($x_1 = 0{\cdot}1558$ and $x_2 = 0{\cdot}1230$). In the figure the scales have been shifted in order to arrive at coinciding enthalpy and temperature coordinates for the lowest point of the homogeneous nematic phase. The temperature scale for mixture x_2 is indicated at the top and for mixture x_1 at the bottom of the figure. In both curves a high as well as a low temperature slope discontinuity, indicating a first order transition, are clearly visible. For the two mixtures a biphasic region extending over a rather large temperature range (about 1·5°C for x_2 and about 0·9°C for x_1) is present in the data. In figure 3 results for the molar heat capacity (in units of the gas constant) as calculated from equation (2) are displayed. Although these two curves are for cooling runs,

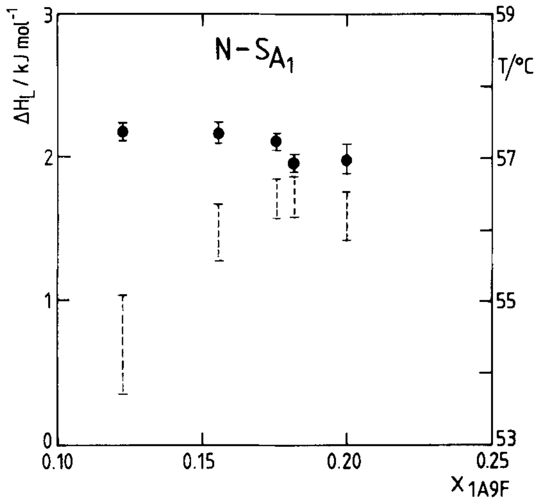

Figure 4. The latent heat (dots) and the width of the biphasic regions (dashed vertical lines) for the N–S_{A_1} transitions of the different mixtures of CCH_4 and 1A9F investigated.

results obtained for heating runs with similar scanning rates are identical. For these two mixtures as well as for the other three investigated, a strong first order transition with a sizeable latent heat is observed. In figure 4 the latent heat and the width of the biphasic region are given as a function of x_{1A9F}. All the mixtures have a latent heat of about 2 kJ/mol, which is, for example, somewhat larger than typical values for nematic–isotropic transitions. It should also be noted that, although the width of the biphasic region decreases on approaching the maximum of the N–S_{A_1} transition curve (see figure 1), it does not shrink to zero at the maximum. This indicates that some impurities must be present in the mixtures. Because of a pretransitional increase in the heat capacity and possibly also because of some rounding-off there is an uncertainty of a few tenths of a degree in the location of the low temperature starting point of the biphasic region (see, e.g., figure 3). For the results displayed in figure 4 we took the beginning of the almost linear C_p behaviour as the low temperature limit of the biphasic region. Thus the widths for this region given in figure 4 are lower limits.

The fact that the N–S_{A_1} phase transition turns out to be first order raises new questions concerning the present theoretical understanding. Indeed on the basis of the Prost model with the two order parameters, characterizing the (normal) density modulation and the antiferroelectric ordering, a second order N–S_{A_1} transition [6, 13] is always found. Only a limited number of N–S_{A_1} transitions for polar molecules with three aromatic rings have been investigated experimentally so far. Enthalpy curves have not been measured but high resolution a.c.–calorimetric heat capacity data are consistent with the predicted second order character. Results have been obtained by Chiang and Garland [14] for heptyloxybenzoyloxycyanostilbene (T7), octyloxybenzoyloxycyanostilbene (T8) and for a mixture of hexylphenylcyanobenzoyloxybenzoate (DB_6) and terephtalbisbutylaniline (TBBA). Recent high resolution X-ray work [15] confirms the second order nature for five mixtures of DB_6 and TBBA. It should, however, be realized that in the Prost model the coupling between the nematic and the (normal) smectic order parameter describing the density modulation has not been included. This should be a valid approximation for systems with large nematic ranges between the isotropic and the smectic phase. If this coupling is included, as for example in the Landau–de Gennes free energy expansion [16], a first order transition between the nematic and any type of smectic A phase can be found, provided the N–S_A transition occurs sufficiently close to the N–I transition. Molecular model calculations by McMillan [17] and Kobayashi [18] predicted that the N–S_A transition can be either first order or second order with a tricritical point, where the transition changes from first to second order, occurring at a certain value of the ratio of the nematic–smectic A transition temperature to the nematic–isotropic transition temperature T_{AN}/T_{NI}. McMillan obtained a universal value of 0·87 for the tricritical T_{NA}/T_{NI} ratio. Experimentally, however, this ratio is much closer to 1. For all systems which have been investigated in sufficient detail, the tricritical T_{NA}/T_{NI} ratio was found to be larger than 0·98 and not universal [19–21]. The largest value for T_{NA}/T_{NI} in our case is 0·94, which applies to the mixture $x_{1A9F} = 0{\cdot}1833$. This is above the McMillan tricritical ratio but well below the experimental values encountered so far. Besides, it should be noted that the values for the latent heat which we observe here are an order of magnitude larger than the values usually measured [19, 20] for first order N–S_A transitions. Only for 4-*n*-heptyloxybenzylidene-4′-*n*-heptylaniline (70·7) was a N–A latent heat (and a N–I latent heat) of about 2 kJ/mol measured [22]. But there the nematic range was only 0·3 K wide. For the mixture $x_{1A9F} = 0{\cdot}1230$ we also find a somewhat larger latent heat than for the $x_{1A9F} = 0{\cdot}1833$ mixture although the McMillan ratio $T_{NA}/T_{NI} = 0{\cdot}93$ is lower. If significant, this difference is opposite to what would be expected. It is also of interest to note that D.S.C. scans for our mixtures indicated that the total enthalpy change associated with N–I transitions was about five times smaller than for N–S_{A_1} transitions. It does not seem very likely therefore that the coupling between the nematic and smectic order parameters is at the origin of the strongly first order N–S_{A_1} transitions in our CCH_4–1AF mixtures. At the moment no clear answer is available for this problem. It should however, be noted that recent U.V. absorption and diamagnetic susceptibility measurements [23] on oriented samples suggest a reorientation of the aminomolecules with regard to the uniaxial director at the N–S_{A_1} transitions. This could be responsible for the strong first order character of those phase changes.

3.2. *The smectic A_1–smectic $\tilde{A}$ transition*

We also carried out a series of heating and cooling runs for the S_{A_1}–$S_{\tilde{A}}$ transition in several CCH_4–1A9F mixtures. Figure 5 gives typical enthalpy results of a cooling run ($\dot{T} \simeq -50$ mK/h) for a mixture with $x_{1A9F} = 0{\cdot}1558$. In order to show more clearly the enthalpy change associated with the phase transition a large linear background $C_p^0(T - T_s)$ with $C_p^0 = 57R$, has been subtracted from the experimental data. On the high temperature side there is a clear slope discontinuity, which could be considered as the onset of the biphasic region of a first order transition. On the low temperature side there is, however, no such discontinuity indicating the end of the biphasic region. This rounding off on the $S_{\tilde{A}}$ side of the transition is also present for heating runs. This can be observed in figure 6 where C_p/R results calculated with equation (2) from the enthalpy data of figure 5 are compared with similar results for a heating run with $\dot{T} \simeq 30$ mK/h. As can be seen in that figure there is rather good agreement between the two sets of data. However, a small downward shift over about 15 mK of the maximum in the C_p/R results of the cooling run can be observed. This small effect was also found for the other mixtures investigated. The rounding off effect

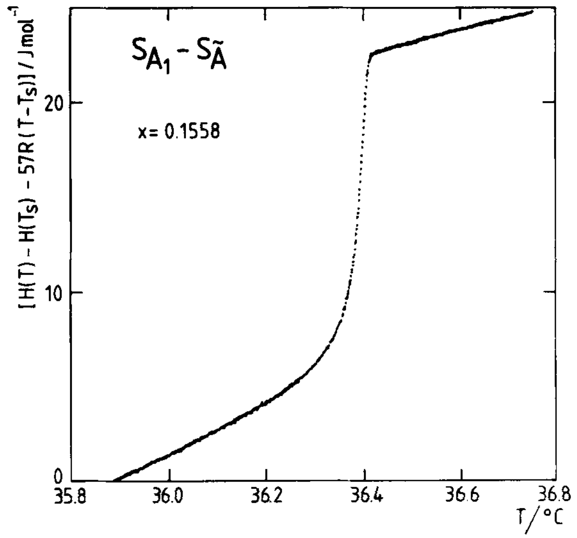

Figure 5. Detailed plot of the enthalpy near the S_{A_1}–$S_{\tilde{A}}$ transition in a mixture of CCH_4 and 1A9F with $x_{1A9F} = 0{\cdot}1558$. Note that for clarity a large linear background $C_p^0\,(T - T_s)$, with $C_p^0 = 57R$, has been subtracted from the experimental data.

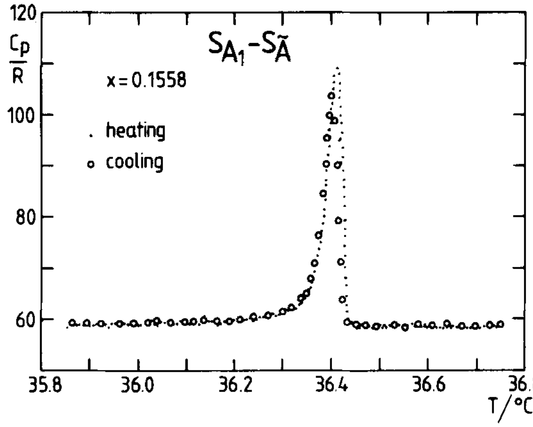

Figure 6. Results for the reduced molar heat capacity C_p/R for a mixture of CCH_4 and 1A9F with the same mole fraction of 1A9F as for figure 5.

in the $S_{\tilde{A}}$ phase is also not caused by the finite scanning rates, because results for a mixture with $x_{1A9F} = 0{\cdot}1833$ for a heating run with $\dot{T} \simeq 5\,\text{mK/h}$ showed a similar, good agreement with the results of a cooling run with $\dot{T} \simeq -30\,\text{mK/h}$. Because of the lack of a clear slope discontinuity on the low temperature side it is not possible therefore to classify with certainty these transitions as first order. However, if we make that assumption we arrive at the results given in figure 7 for the enthalpy change associated with the S_{A_1}–$S_{\tilde{A}}$ transition in the different mixtures. The two pluses in that figure represent results obtained with differential scanning calorimetry. The D.S.C. results for $x_{1A9F} = 0{\cdot}1833$ was shifted to the same value as obtained from our adiabatic measurement (solid dot) for that concentration, and considered as a calibration measurement for the low concentration ($x_{1A9F} = 0{\cdot}107$) D.S.C. result. The

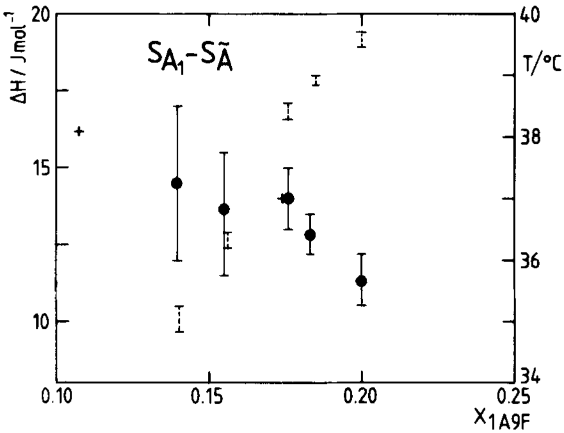

Figure 7. Enthalpy changes (dots) and temperature widths (dashed vertical lines) associated with the smectic A_1 to smectic $\tilde{A}$ phase transition of the different mixtures of CCH_4 and 1A9F investigated.

enthalpy changes associated with the S_{A_1}–S_{A_2} transitions are of the order of 15 J/mol and seem to decrease somewhat with increasing mole fraction of 1A9F.

The enthalpy changes are rather small and could easily be accounted for by fluctuation effects associated with a second order transition. Since the presence of a biphasic region cannot be established with certainty we also have to consider this possibility. Assuming the transition to be second order we analysed the C_p/R data in terms of the power laws,

$$C_p/R = A\varepsilon^{-\alpha} + B + D\varepsilon, \quad \text{for } T > T_c, \tag{3}$$

$$C_p/R = A'|\varepsilon|^{-\alpha'} + B' + D'\varepsilon, \quad \text{for } T < T_c, \tag{4}$$

with T_c the second order critical temperature and $\varepsilon = (T - T_c)/T_c$. However from looking at the data of figure 6 it should be immediately clear that above T_c the power law fits are not possible because there is no pretransitional heat capacity increase present in the data. Several fits to the data below T_c have been attempted with different kinds of combinations of adjustable or imposed parameters in equation (4). In all cases large χ_ν^2 values and systematic deviations were obtained. In parts (*a*)–(*c*) of figure 8 typical fitting results (the solid curves) are compared with the experimental results (dots) for the mixture with $x_{1A9F} = 0{\cdot}1761$. In the table the corresponding parameter values are given. These fits have been carried out with $D' = 0$. For the given temperature range of the data, including a linear term did not make any difference. In part (*d*) of figure 8 a different kind of fit to the same data is given.

Parameter values from fits to the C_p/R data below the smectic A_1 to smectic $\tilde{A}$ transition with equation (4) ($D' = 0$) for the mixture $x_{1A9F} = 0{\cdot}1761$.

Fit	T_c/°C	α'	A'	B'
(*a*)	(38·48)†	1·29	$1{\cdot}25 \times 10^{-4}$	56·94
(*b*)	(38·47)	0·63	0·048	53·29
(*c*)	38·470	(0·50)	0·20	49·89

† Parameter values in parentheses indicate that the parameter was held constant at the quoted value.

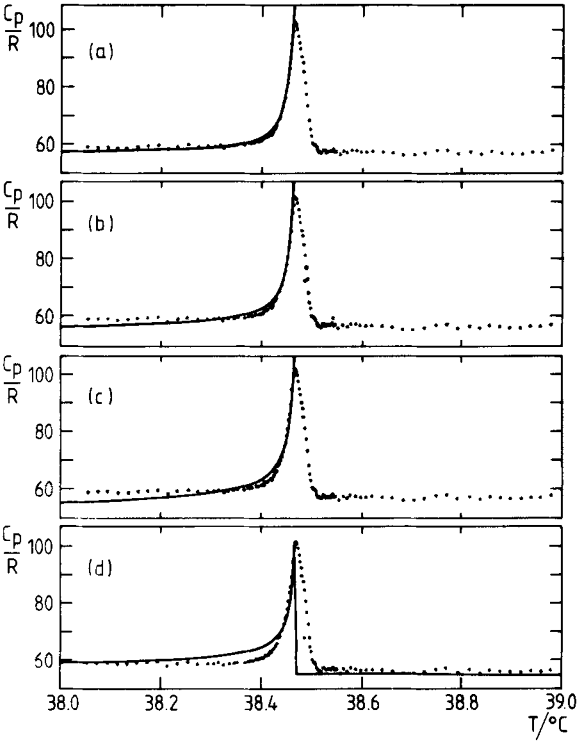

Figure 8. Comparison between the results of different fitting procedures (solid curves) and experimental data (dots) for a mixture of CCH_4 and 1A9F with $x_{1A9F} = 0{\cdot}1761$. See the text for details.

Because the temperature dependence of our C_p data for the S_{A_1}–$S_{\tilde{A}}$ transition shows some qualitative similarity with the C_p behaviour near the second order smectic A to smectic C transitions [22, 24–28], we also tried fits with an expression proposed by Huang and Viner [26] for the S_A–S_C transition. On the basis of a Landau free energy expansion up to a sixth order term in the tilt order parameter Huang and Viner arrived at the following equations for the heat capacity:

$$C_p/R = C_p^0/R, \qquad \text{for } T > T_c, \tag{5}$$

$$C_p/R = C_p^0/R + A\frac{T}{T_c}\left(\frac{T_m - T_c}{T_m - T}\right)^{1/2}, \qquad \text{for } T < T_c. \tag{6}$$

The background heat capacity C_p^0 results from the regular part of the free energy, and the adjustable parameters, A and T_m, are related to the coefficients in the free energy expansion [26]. For tricritical points the coefficient of the fourth order term is zero, and equation (6) reduces to the simple power law expression given by equation (4) with $\alpha' = 0{\cdot}5$. Such a fit, with $\alpha' = 0{\cdot}5$ imposed, corresponds to part (*c*) of figure 8. In part (*d*) of figure 8 the results of a fit with equation (6) are given. The parameter values are: $T_c = 38{\cdot}467$°C, $A = 82{\cdot}5$, $C_p^0/R = 55{\cdot}64$ and $T_m = 38{\cdot}468$°C. This kind of fit also does not describe the data very well. Indeed it appears impossible to describe the data properly with power law type expressions. We believe this is because the observed C_p anomaly is mainly the result of a smeared-out first order transition with a small latent heat. This does not exclude a contribution of a fluctuation induced pretransition increase in the $S_{\tilde{A}}$ phase. The observation that cooling runs show a C_p maximum about 10 to 20 mK lower than corresponding heating runs also indicates a small first order hysteresis effect.

So far, only one other S_{A_1}–$S_{\tilde{A}}$ phase transition has been investigated calorimetrically in detail. Huang *et al.* [29] carried out high resolution a.c.–calorimetric measurements of the temperature dependence of the heat capacity near the S_{A_1}–$S_{\tilde{A}}$ transition for the pure triaromatic compound 4-*n*-heptylphenyl-4′-(4″-nitrobenzoyloxy)benzoate ($DB7NO_2$). In comparing their C_p results with ours we notice some important qualitative differences. Although their heat capacity anomaly is relatively asymmetric, there is a clear pretransitional increase in the S_{A_1} phase over about 0·5°C, an effect completely absent in our data. The $DB7NO_2$ data above and below T_c could be fitted reasonably well with the power law expressions (3) and (4) with $\alpha = \alpha' = 0{\cdot}37$, $A/A' = 0{\cdot}26$ under the imposed condition $D = D'$ but allowing for a 5 per cent jump at the transition between B and B'. This heat capacity discontinuity and the fact that there existed about 10 mK hysteresis in the peak position of the heat capacity anomalies between several successive cooling and heating runs was considered as an indication for a weakly first order contribution. Because the values $\alpha = \alpha' = 0{\cdot}37$ and $A/A' = 0{\cdot}26$ are not too far away from those obtained near the ^3He–^4He tricritical point [30] the authors suggested that the S_{A_1}–$S_{\tilde{A}}$ transition in $DB7NO_2$ may be very close to a tricritical point, similar to that found in the ^3He–^4He mixture.

In our data we do not find evidence for a nearly tricritical point, but the suggestion of a weak, first order transition for $DB7NO_2$ is in accord with our results for the CCH_4–1A9F mixtures. A first order S_{A_1}–$S_{\tilde{A}}$ transition is not in conflict with the mean field predictions of the Prost model. Indeed, according to the calculations by Prost and Barois [6] the S_{A_1}–$S_{\tilde{A}}$ transition line can be second order in one part of a phase diagram, pass through a tricritical point and become first order for another part of the phase diagram. Because of the continuous degeneracy of directions for the spatial modulation of the $S_{\tilde{A}}$ phase the order parameter fluctuations occur on a cone in k space (as for the nematic to smectic C transition) and the transition is expected [13, 31] to be first order on the basis of arguments presented by Brazovskii [32]. This would certainly be consistent with the smallness of the observed transition enthalpies for our CCH_4–1A9F mixtures.

4. Summary and conclusions

In this paper we have presented experimental data for the phase diagram and for the enthalpy and the heat capacity in a frustrated smectic system exhibiting smectic A polymorphism (smectic A_1 and smectic $\tilde{A}$) at low temperatures. Both the nematic to smectic A_1 and the smectic A_1 to smectic $\tilde{A}$ phase transitions have been investigated in detail by adiabatic scanning calorimetry for several binary mixtures of 4-cyanocyclohexyl-4′-*n*-butylcyclohexane and 1-amino-9-fluorenone.

For all the mixtures investigated, the N–S_{A_1} transition is observed to be first order with latent heat values of about 2 kJ/mol. The fact that this transition is first order with a large latent heat is not consistent with present theoretical insight for this type of phase transition. On the basis of the Prost model [4, 5] with two order parameters, one for the density modulation and one for the ferroelectric ordering, a second order N–S_{A_1} transition [6, 13] is always found. Thus one might have to look for a coupling with another order parameter. An obvious possibility would be the coupling between the nematic order parameter and the (normal) order parameter for the density modulation [16–18]. As pointed out in § 3.1 all the mixtures have a sizeable nematic range and it is not very likely that the N–S_A coupling is at the origin of the large latent heat. Possibly the reorientation of the aminomolecules [23] at the N–S_{A_1} transition could be responsible for the observed calorimetric behaviour.

The enthalpy change observed at the S_{A_1}–$S_{\tilde{A}}$ transition is two orders of magnitude smaller than for the N–S_{A_1} transition. Because of rounding off effects in the calorimetric data, the order of the transition could not be determined unambiguously. However, the analysis of the data presented in § 3.2 strongly points in the direction of a weakly first order S_{A_1}–$S_{\tilde{A}}$ transition. This would be consistent with theoretical expectations for this transition [13, 31].

We wish to thank J. Prost and W. Van Dael for helpful discussions.

References

[1] Sigaud, G., Hardouin, F., and Archard, M. F., 1979, *Physics Lett.*, **72A**, 24.
[2] Hardouin, F., Levelut, A. M., Archard, M. F., and Sigaud, G., 1983, *J. Chim. phys.*, **80**, 53, and references therein.
[3] Nguyen Huu Tinh, 1983, *J. Chim. phys.*, **80**, 83.
[4] Prost, J., 1979, *J. Phys., Paris*, **40**, 581.
[5] Prost, J., 1980, *Proceedings of the Conference on Liquid Crystals of One- and Two-Dimensional Order*, Garmisch Partenkirchen (Springer Verlag), p. 125.
[6] Prost, J., and Barois, P., 1983, *J. Chim. phys.*, **80**, 65.
[7] Barois, P., Prost, J., and Lubensky, T. C., 1985, *J. Phys., Paris*, **46**, 391.
[8] Sigaud, G., Archard, M. F., Hardouin, F., and Gasparoux, H., 1985, *J. Phys. Lett., Paris*, **46**, 321.
[9] Kasting, G. B., Garland, C. W., and Lushington, K. J., 1980, *J. Phys., Paris*, **41**, 879.
[10] Thoen, J., Marijnissen, H., and Van Dael, W., 1982, *Phys. Rev.* A, **26**, 2886.
[11] Thoen, J., Bloemen, E., Marijnissen, H., and Van Dael, W., 1982, *Proceedings of the 8th Symposium of Thermophysical Properties*, National Bureau of Standards, Maryland, 1981 (American Society of Mechanical Engineers), p. 422.
[12] Marijnissen, H., Thoen, J., and Van Dael, W., 1983, *Molec. Crystals liq. Crystals*, **97**, 149.
[13] Prost, J., 1984, *Adv. Phys.*, **33**, 1.
[14] Chiang, C., and Garland, C. W., 1985, *Molec. Crystals liq. Crystals*, **122**, 25.
[15] Chan, K. K., Pershan, P. S., and Sorensen, L. B., 1986, *Phys. Rev.* A, **34**, 1420.
[16] de Gennes, P. G., 1974, *The Physics of Liquid Crystals* (Clarendon).
[17] McMillan, W. L., 1971, *Phys. Rev.* A, **4**, 1238.
[18] Kobayashi, K. K., 1970, *Physics Lett.*, **31A**, 125; 1970, *J. phys. Soc. Japan*, **29**, 101.
[19] Thoen, J., Marynissen, H., and Van Dael, W., 1984, *Phys. Rev. Lett.* **52**, 204.
[20] Marynissen, H., Thoen, J., and Van Dael, W., 1985, *Molec. Crystals liq. Crystals*, **124**, 195.
[21] Ocko, B. M., Birgeneau, R. J., and Litster, J. D., 1986, *Z. Phys.* B, **62**, 487, and references therein.
[22] Thoen, J., and Synhaeve, G., 1985, *Molec. Crystals liq. Crystals*, **127**, 229.
[23] Sigaud, G., and Auguste, J. M. (unpublished results).
[24] Birgeneau, R. J., Garland, C. W., Kortan, A. R., Litster, J. D., Meichle, M., Ocko, B. M., Rosenblatt, C., Yu, L. J., and Goodby, J., 1983, *Phys. Rev.* A, **27**, 1251.
[25] Meichle, M., and Garland, C. W., 1983, *Phys. Rev.* A, **27**, 2624.
[26] Huang, C. C., and Viner, J. M., 1982, *Phys. Rev.* A, **25**, 3385.
[27] Huang, C. C., and Lien, S. C., 1981, *Phys. Rev. Lett.*, **47**, 1917.
[28] Lien, S. C., Viner, J. M., Huang, C. C., and Clark, N. A., 1983, *Molec. Crystals liq. Crystals*, **100**, 145.
[29] Huang, C. C., Lien, S. C., Dumrongrattana, S., and Chiang, L. Y., 1984, *Phys. Rev.* A, **30**, 965.
[30] Islander, S. T., and Zimmermann, W., Jr., 1973, *Phys. Rev.* A, **7**, 188.
[31] Wang, J., and Lubensky, T. C., 1984, *J. Phys., Paris*, **45**, 1653.
[32] Brazovskii, S. A., 1975, *Soviet Phys. JETP*, **47**, 85.